Available online at www.sciencedirect.com
ScienceDirect
International Journal of Mass Spectrometry 269 (2008) 95–100
International Journal of Mass Spectrometry
www.elsevier.com/locate/ijms

Cluster ion formation of alkali halides by electrospray droplet impact

Kunihiko Mori, Kenzo Hiraoka *

Clean Energy Research Center, University of Yamanashi, Takeda-4, Kofu 400-8511, Japan

Received 5 September 2007; received in revised form 20 September 2007; accepted 20 September 2007
Available online 2 October 2007

Abstract

Positive and negative cluster ions formed by electrospray droplet impact on the alkali halides (MX) were measured for all alkali halides. Small amounts of powder samples deposited and crushed into thin films on the metal substrate were served for the measurement. The size distribution of cluster ions is very limited for LiF, CsF, and LiI. Little or no fluoride cluster ions $F^-(MF)_n$ were detected. In general, distribution of n for negative cluster ions $X^-(MX)_n$ is narrower than that for positive cluster ions $M^+(MX)_n$, probably due to the instability caused by the mutual Coulomb repulsion between the larger-size halide ions than alkali ions. While the cubic-like structures are preferred for alkali halides with smaller ionic radii, the stacked hexagonal structures with $n = 3$, 6, and 9 are preferred for those with larger ionic radii.

Keywords: Alkali halide; Electrospray droplet impact; Cluster ion; SIMS

1. Introduction

Mass spectrometric studies of gas-phase cluster ions of alkali halides have been widely investigated because of their elementary properties. Honda et al. studied the mechanism of cluster formation during ion bombardment of alkali halides and found the secondary ion clusters of $Na^+(NaF)_{13}$ and $Cs^+(CsI)_3$ [1]. Campana et al. examined the effect of cluster surface energies on secondary-ion-intensity distributions from ionic crystals. They observed ultra-high mass cluster ions ($m/z > 18{,}000$) of $Cs^+(CsI)_n$ by xenon-ion bombardment on CsI crystal. The mass spectra (ion intensity vs. n) show anomalous behavior which is correlated with hypothesized dominance of cubic-like clusters having low surface energies, e.g., appearance of magic numbers at $n = 4$, 6, 9, 13, 16, 22, 25, 37, 44, 46, and 62 [2]. However, they did not detect negative ions $I^-(CsI)_n$ greater than $n = 4$. Martin calculated relative stability of clusters having the composition of $Na^+(NaCl)_n$ and found that $Na^+(NaCl)_4$ is a particularly stable charged cluster [3]. He also predicted that the most stable $Na^+(NaCl)_6$ configuration among structural isomers resembled dual hexagonal rings with a single sodium atom centered above one ring and that the corresponding neutral clusters (i.e., $(NaCl)_n$ for $n = 6$, 9, 12) are stable in the stacked hexagonal ring configurations. Barlak et al. investigated secondary ion mass spectrometry of alkali iodides [4–6] using Ar^+ beam. The structures of cluster ions at certain n values, which have enhanced ion intensities, were postulated to have cubic-like atomic arrangements which are reminiscent of the bulk crystal structure. Dunlap studied a simple nearest neighboring bond breaking model (BBM) of secondary ion mass spectrometry and predicted the major deviations from the smooth envelope ($n = 13$, 22, 37, and 62 for $M^+(MX)_n$) due to the dominance in the SIMS spectra of cubic-like clusters having the lowest ratio of broken bonds [7].

It should be noted that anomaly in peak abundances for $M^+(MX)_n$ has been clearly observed when a double-focusing (Mattauch–Herzog geometry) mass analyzer was used [2–4]. In the sector-field mass spectrometer, cluster ions requires hundred μs to traverse the instrument. If the ions decompose within that time they are not observed as intact ions. By contrast, cluster ions in a linear time of flight mass spectrometer need only enough time to be fully accelerated in order to appear at its original mass numbers; subsequent decays simply increase the width of the peak since the velocity of the center of mass remains constant. Thus the fragment ions are still detected at the approximate position of the parent ion. In fact, Ens et al.

* Corresponding author.
E-mail address: hiraoka@yamanashi.ac.jp (K. Hiraoka).

1387-3806/$ – see front matter © 2007 Elsevier B.V. All rights reserved.
doi:10.1016/j.ijms.2007.09.013

found no anomalies in intensity distributions of $Cs^+(CsI)_n$ in Cs^+ ion SIMS when they used a linear time-of-flight mass spectrometer [8]. In their system, the cluster ions are accelerated to their full energies of 10 keV in 0.17 μs, and so their measurement yielded the population after their production. This clearly indicates that the anomaly in the population of the disintegration is due to the decomposition of primary metastable cluster ions at least a few μs after their birth by the primary ion impact. Martin suggests that particularly stable cluster ions are observed when energy barriers prevent unimolecular dissociation via the emission of ions, atoms, or simple molecules [3].

Katakuse et al. measured ultra-high-mass spectra of CsI clusters $Cs^+(CsI)_n$ up to $n = 210$ and they obtained evidence for the existence of stable neutral cubic-like structures with even number of atoms [9]. They found that the intensity behavior of the clusters for $n < 30$ agreed with the earlier results [2,4–6]. However, in the high mass region, the ion intensity varied smoothly and local maxima and minima were observed. The cluster sizes at local maxima were not equal to the *n*-values of cluster ions of cubic-like structures but those at local minima roughly correspond to the cubic-like structures in the high mass region. A possible explanation for these results is that the positively charged clusters decay to stable neutral rectangular clusters by the emission of small positive fragments or grow to larger stable neutral clusters by the attachment of small negative clusters.

Alkali halide cluster ions have been produced so far by using such methods as low-energy electron beam [10], laser vaporization [11,12], and fast-atom bombardment [1,2,4–6,8,9,13]. The negatively charged cluster ions generated by these methods were relatively weaker than positively charged ones and information on the stabilities of natively charged cluster ions are thus relatively scarce. Recently, we have developed electrospray droplet impact/SIMS (EDI/SIMS). It was found that EDI is most suitable for the observation of negative ions as well as positive ions. This may be due to the fact that the secondary electrons generated are confined in the colliding interface between the impacting projectile and the solid sample and they are eventually detected as negative ions. In this study, positive and negative cluster ions for all alkali halides are measured. Somewhat smaller but similar "magic numbers" are observed for negative cluster ions as for positive ones with some exceptions.

2. Experimental

The general experimental procedures were similar to those described previously [14–17]. The charged liquid droplets formed by electrospraying 1 M acetic acid aqueous solution at atmospheric pressure are sampled through an orifice with a 400 μm diameter into the first vacuum chamber, transported into a first quadrupole ion guide, and accelerated by 10 kV after exiting the ion guide. The *m*/*z* values of the primary droplet projectiles selected by the first ion guide are approximately in the range of 1×10^4 to 5×10^4, as estimated by the frequency and the amplitude of radiofrequency applied to the first ion

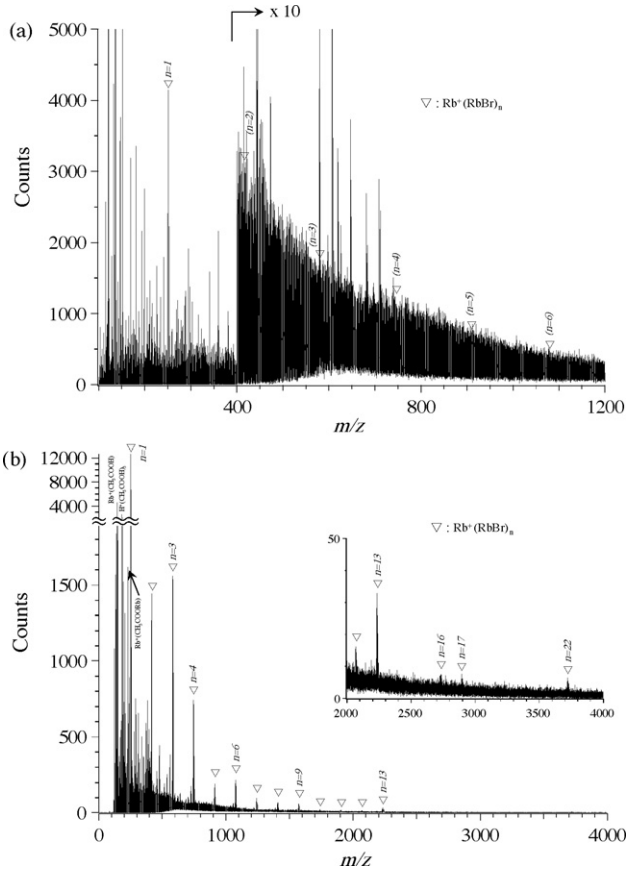

Fig. 1. Positive EDI mass spectra for RbBr. (a) 1 μL of 10^{-3} M RbBr aqueous solution deposited/dried on the stainless steel substrate with a diameter of 3 mm. (b) A small amount of RbBr powder crushed into a very thin deposit on the stainless steel substrate using a spatula.

guide. The values of *m* and *z* which give *m*/*z* values of 10^4 and 5×10^4 are estimated to be $m = 6 \times 10^5$ *u* and $z = 62$, and $m = 1.6 \times 10^7$ *u* and $z = 311$, respectively [17]. Diameters for the water droplets are calculated to be 5 and 14 nm, respectively. The kinetic energy of a projectile, for example, with $z = 100$ charges (e.g., $[(H_2O)_{90000} + 100H]^{100+}$) with mass of $\sim 1.6 \times 10^6$ *u* (the charged droplet at the Rayleigh limit) is 1×10^6 eV for the acceleration potential of 10 kV. The electrospray droplets (i.e., the multiple-charge massive cluster ions) impact on a sample deposited on the stainless steel substrate. The secondary ions formed by the projectile droplet impact are transported into a second quadrupole ion guide for collisional cooling and mass-analyzed by an orthogonal time-of-flight mass spectrometer (Accu-TOF, JEOL, Akishima, Tokyo). The transit time of the cluster ions in the second ion guide is ~1 ms. The nascent cluster ions generated by EDI suffer from multiple collisions with N_2 buffer gas in the second ion guide and the more stable cluster ions are preferentially formed by the degradation of metastable larger cluster ions. The measurement of mass spectra was made using a pulse-counting system.

In the previous investigations [1,2,6,8,9,11–13], positively charged cluster ions $M^+(MX)_n$ with M = Na and Cs for all X (F, Cl, Br, and I) [2,8,9,11,13], and MI for all M(Li, Na,

Table 1
Magic numbers observed for MX

		F	Cl	Br	I
Li	$Li^+(LiX)_n$	3, 4 /4	3, 4 /4	3 /4	3 /3
	$X^-(LiX)_n$	–/2	4, 12 /13	4, 12 /12	4 /9
Na	$Na^+(NaX)_n$	4, 13, 16, 17, 22, 25, 28, 31, 34, 37 /37	3, 13, 16, 22 /22	13, 22 /22	3, 6, 13, 16, 22, 25, 31, 34, 37 /37
	$X^-(NaX)_n$	–/2	3, 13 /13	4, 9, 13 /13	4, 9, 31 /31
K	$K^+(KX)_n$	4, 9, 13, 16, 17, 22, 28, 31, 34, 37 /37	4, 9, 13, 16, 17, 22 /22	3, 6, 9, 13, 16, 17, 22, 37 /37	3, 6, 9, 13, 16, 22 /22
	$X^-(KX)_n$	–/1	3, 4, 9, 13, 16, 17, 22 /22	3, 4, 9, 13, 16, 17, 22 /22	3, 9, 13, 16, 22 /22
Rb	$Rb^+(RbX)_n$	3, 4, 9, 13, 17, 22 /22	3, 4, 9, 13, 16, 17, 22 /22	3, 4, 6, 9, 13, 16, 17, 22 /22	3, 4, 6, 9, 13, 16, 17, 22 /22
	$X^-(RbX)_n$	–/1	3, 4, 6, 9, 13 /13	3, 4, 6, 9, 13 /13	3, 4, 6, 9, 13, 16, 17, 22 /22
Cs	$Cs^+(CsX)_n$	3, 4 /4	3, 4, 6, 9, 13, 16, 22 /22	3, 6, 9, 13, 16, 17, 22 /22	3, 4, 6, 9, 13, 16, 17, 22, 25, 28, 31, 37 /37
	$X^-(CsX)_n$	–/–	3, 6, 9, 13 /13	3, 6, 9, 13, 16, 17, 22 /22	3, 4, 6, 9, 13, 22 /22

The symbol "–" denotes that no magic number was detected. The number of denominator denotes the maximum number of the cluster ion observed.

K, Rb, and Cs) [4,5,18,19], and negatively charged cluster ions, $Cl^-(NaCl)_n$ [11,12], $Cl^-(CsCl)_n$ [11], $I^-(NaI)_n$ [11] and $I^-(CsI)_n$ [11] have been studied. In this work, measurements of positive and negative cluster ions of $M^+(MX)_n$ and $X^-(MX)_n$ for all the combination of M and X were made.

In the measurement of EDI mass spectra, a small amount of alkali halide powder was put on the stainless steel substrate and it was crushed into a very thin deposit using a spatula. The residual powder was blown off in order to prevent the contamination of the vacuum system.

The suppliers for the alkali halide reagents are as follows. Kanto Chemical, Co. Inc. (Tokyo, Japan): LiBr, LiI, NaI, KF, KBr, RbCl, RbI, CsF, CsCl, CsBr, and CsI. Wako Pure Chemical Industries, Ltd. (Osaka, Japan): Lif and LiCl. Sigma–Aldrich, Inc. (St. Louis, MO, USA): NaBr. Sigma–Aldrich, Inc. Japan (Tokyo, Japan): NaCl. Nakarai Tesque, Inc. (Kyoto, Japan): KI. Strem Chemicals, Inc. (Newburyport, MA, USA): RbF and RbBr. Alfa Aesar, A Johnson Matthey Company (Ward Hill, MA, USA): NaF. Merk, Ltd. (Darmstadt, Germany): KCl.

3. Results and discussion

It was found that the EDI mass spectra are highly dependent on the sample preparation. When the aqueous solutions of alkali halides were deposited/dried on the stainless steel substrate, the ion abundances of cluster ions were very weak and large-size cluster ions could not be observed. In contrast, much stronger ion signals and also much wider size distribution of cluster ions could be observed for the powder sample crushed into very fine deposit on the metal substrate. As an example, Fig. 1(a) shows the positive-mode EDI mass spectrum for RbBr prepared by drying the 1 μL of the aqueous solution of 1×10^{-3} M RbBr and Fig. 1(b) by crushing the solid powder to form a very thin deposit on the stainless steel substrate. In the mass spectrum prepared from the aqueous solution, only $Rb^+(RbBr)_n$ with $n = 1$ is observed but none for $n \geq 2$. Besides, lots of peaks originating from impurities contaminated during the sample preparation appear in the mass spectrum. This is due to the enrichment of impurities on the surface of the crystal during the crystallization of salt from saturated aqueous solution. In contrast, the mass

Table 2
All kinds of cluster ions observed by EDI are summarized together with the maximum sizes of $M^+(MX)_n$ and $X^-(MX)_n$ detected

	Positive cluster ions		Negative cluster ions	
LiF	$Li^+(CH_3COOH)_{0–2}(CH_3COOLi)_{0–3}$	$Li^+(LiF)_4$	$F^-(CH_3COOH)(CH_3COOLi)_{0–1}$	$F^-(LiF)_2$
LiCl	$Li^+(CH_3COOH)_{0–2}(CH_3COOLi)_{1–3}Li^+(LiCl)(CH_3COOH)_{1–2}$	$Li^+(LiCl)_4$	$CH_3COO^-(LiCl)_{1–12}$	$Cl^-(LiCl)_{13}$
LiBr	$Li^+(LiBr)_{0–1}(CH_3COOLi)_{1–4}Li^+(LiBr)_{0–2}(CH_3COOH)_{1–4}$	$Li^+(LiBr)_4$	$Br^-(LiBr)_{1–9}(CH_3COOLi)$	$Br^-(LiBr)_{12}$
LiI	$Li^+(CH_3COOLi)_{1–11}Li^+(LiI)_{1–8}(CH_3COOLi)_{1–9}$	$Li^+(LiI)_3$	$I^-(CH_3COOLi)_{1–5}I^-(LiI)(CH_3COOLi)_{1–6}$	$I^-(LiI)_9$
NaF	$Na^+(CH_3COONa)_{1–6}(NaF)_{1–11}$	$Na^+(NaF)_{37}$	$F^-(CH_3COONa)_{1–14}CH_3COO^-(CH_3COONa)_{1–14}$	$F^-(NaF)_2$
NaCl	$Na^+(CH_3COOH)_{0–3}$	$Na^+(NaCl)_{22}$	–	$Cl^-(NaCl)_{13}$
NaBr	$Na^+(NaBr)_{0–8}(CH_3COONa)$	$Na^+(NaBr)_{22}$	$Br^-(NaBr)_{2–3}(CH_3COONa)$	$Br^-(NaBr)_{13}$
NaI	$Na^+(CH_3COONa)(NaI)_{1–36}$	$Na^+(NaI)_{37}$	$CH_3COO^-(NaI)_{1–27}$	$I^-(NaI)_{31}$
KF	$K^+(KF)_{0–3}(CH_3COOK)_{0–3}$	$K^+(KF)_{37}$	$F^-(CH_3COOK)_{1–10}CH_3COO^-(CH_3COOK)_{0–9}$	$F^-(KF)$
KCl	$K^+(CH_3COOK)/K^+(KCl)_{22}$	$K^+(KCl)_{22}$	$CH_3COO^-(KCl)$	$Cl^-(KCl)_{22}$
KBr	$K^+(KBr)_{2–7}(CH_3COOK)$	$K^+(KBr)_{37}$	$Br^-(KBr)(CH_3COOK)$	$Br^-(KBr)_{22}$
KI	$K^+(KI)_{0–8}(CH_3COOK)$	$K^+(KI)_{22}$	$CH_3COO^-(KI)_{1–3}$	$I^-(KI)_{22}$
RbF	$Rb^+(RbF)_{0–2}(CH_3COORb)_{0–3}$	$Rb^+(RbF)_{22}$	$CH_3COO^-(CH_3COORb)_{1–2}$	$F^-(RbF)$
RbCl	$Rb^+(CH_3COORb)$	$Rb^+(RbCl)_{22}$	$CH_3COO^-(CH_3COORb)$	$Cl^-(RbCl)_{13}$
RbBr	$Rb^+(CH_3COORb)$	$Rb^+(RbBr)_{22}$	$CH_3COO^-(RbBr)$	$Br^-(RbBr)_{13}$
RbI	$Rb^+(RbI)_{0–4}(CH_3COORb)_{1–2}$	$Rb^+(RbI)_{22}$	$CH_3COO^-(RbI)$	$I^-(RbI)_{22}$
CsF	$Cs^+(CH_3COOCs)_{1–6}$	$Cs^+(CsF)_4$	$CH_3COO^-(CH_3COOCs)_{1–9}$	–
CsCl	$Cs^+(CsCl)_{0–5}(CH_3COOCs)$	$Cs^+(CsCl)_{22}$	$Cl^-(CH_3COOCs)$	$Cl^-(CsCl)_{13}$
CsBr	$Cs^+(CH_3COOCs)$	$Cs^+(CsBr)_{22}$	$Br^-(CsBr)_{0–9}(CH_3COOCs)$	$Br^-(CsBr)_{22}$
CsI	$Cs^+(CsI)_{0–8}(CH_3COOCs)$	$Cs^+(CsI)_{37}$	$I^-(CsI)_{0–3}(CH_3COOCs)$	$I^-(CsI)_{22}$

spectrum obtained from the crushed sample is much simpler and cluster ions of $Rb^+(RbBr)_n$ up to $n = 22$ are observed. The ejection of a compact cluster from a perfect crystal face (direct emission) can occur, but it involves the breaking of a large number of bonds [13]. Furthermore, the finite energy of the primary particle alone limits the size of clusters that can be ejected [20]. In contrast, sputtering of nano-chunks can take place from the rough surface due to the energy stored in defects and surface topography [21,22].

In Fig. 1(b), abundance anomaly was observed at $n = 3$, 4, 6, 9, 13, 16, 17, and 22. This indicates that the cluster ions $Rb^+(RbBr)_n$ with these n are more stable compared to the neighboring cluster ions and are preferentially observed by EDI. Table 1 summarizes the magic numbers observed for all alkali halides. In general, the magic numbers observed for MX in Table 1 are in good agreement with the available data reported previously [1,2,4–6,8–13,18,19]. In the present work, the alkali halide samples were bombarded by the water droplet containing 1 M acetic acid. Upon collision, the surface of the solid alkali halide was exposed by the shock wave-excited selvedge in the colliding interface. As a result, not only alkali halide cluster ions but also many kinds of mixed clusters of M^+ and X^- containing CH_3COOH, CH_3COOM, etc. are formed as secondary ions. In Table 2, all kinds of cluster ions observed by EDI are summarized together with the maximum sizes of $M^+(MX)_n$ and $X^-(MX)_n$ detected.

Table 3
Lattice energies for MX in kJ/mol [23]

	F	Cl	Br	I
Li	1030	834	788	730
Na	910	769	732	682
K	808	701	671	632
Rb	774	680	651	617
Cs	744	657	632	600

As shown in Table 1, only small-size positive and negative cluster ions are observed for LiF. This may be mainly due to the highest lattice energy of LiF (1030 kJ/mol in Table 3) [23] among all alkali halides. For positive cluster ions, "magic numbers"

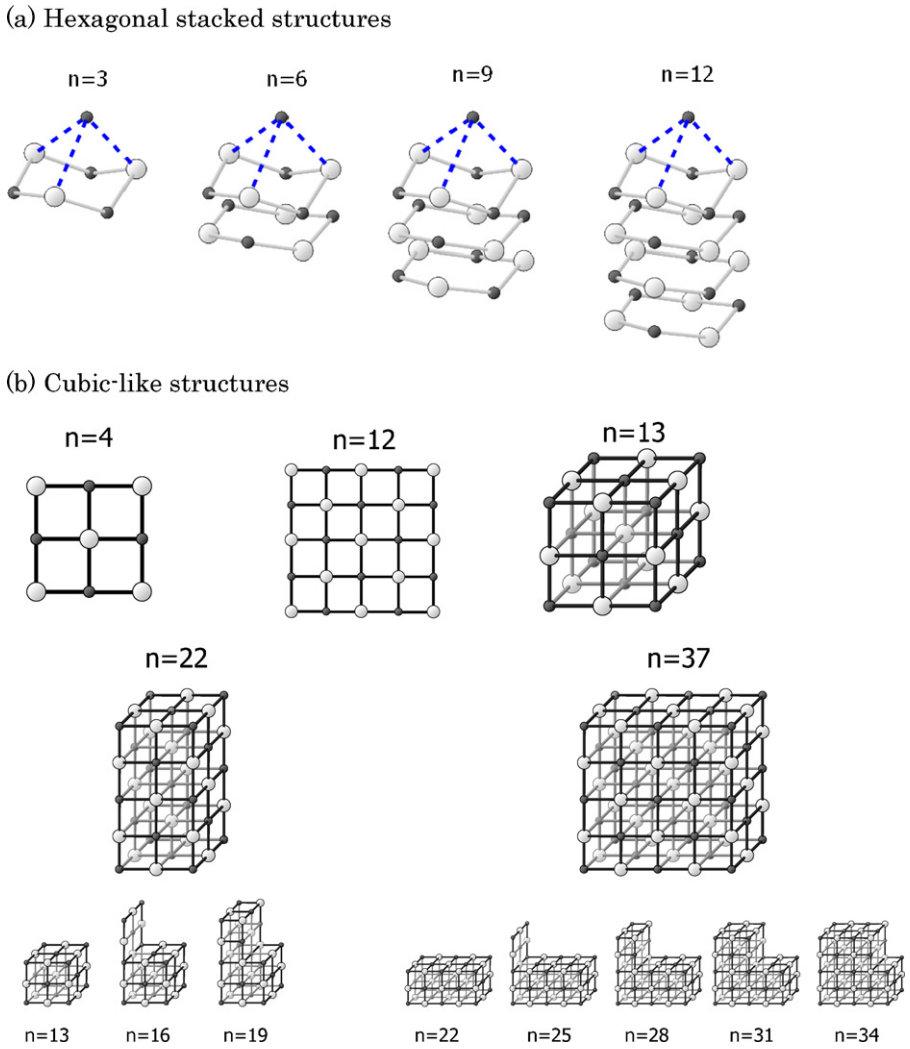

Fig. 2. The postulated hexagonal structures (a) and cubic-like structures (b) for $M^+(MX)_n$ and $X^-(MX)_n$ cluster ions. The hexagonal ring structures have a bent conformation [3]. The structures shown are only simplified and conceptual models and should not be regarded as the most stable configurations.

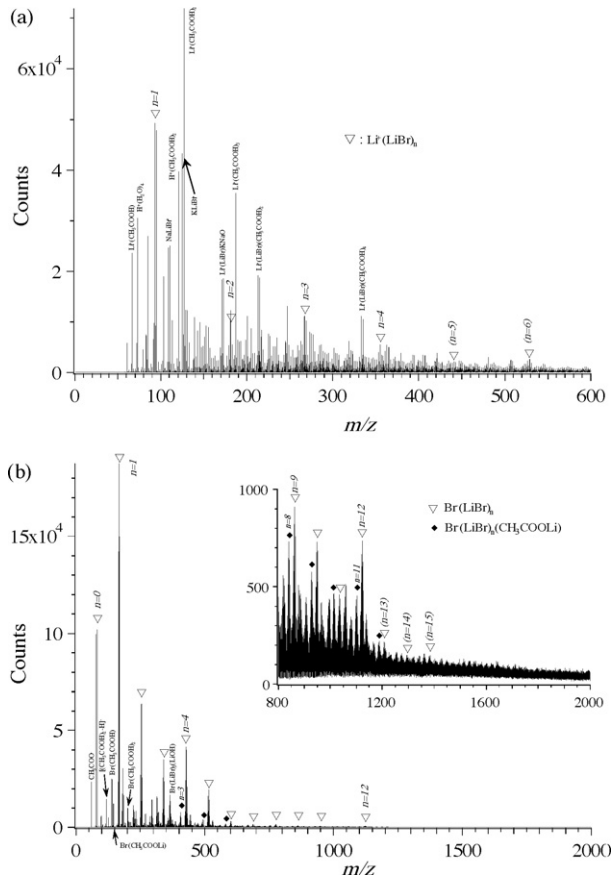

Fig. 3. Positive- and negative-mode EDI mass spectra for LiBr.

$n = 3$ for all LiX and 4 for LiF and LiCl are observed. The magic number 3 has been explained by the hexagonal ring with an additional M^+ ion above its plane (see Fig. 2) [4]. Magic number 4 is most likely to have ($3 \times 3 \times 1$) planar structure (Fig. 2). For negative cluster ions $X^-(LiX)_n$ in Table 1, magic numbers of 4 and/or 12 are recognized. The magic number of $n = 12$ observed for negative cluster ions of LiCl and LiBr (Fig. 3) is worthwhile noting. The cluster for $n = 12$ may be tentatively explained by the planar structure of ($5 \times 5 \times 1$) [8] and/or hexagonal stacked structure shown in Fig. 2. The absence of magic numbers of $n = 3$, 6, and 9 may suggest that the planar ($5 \times 5 \times 1$) structure is more likely for $X^-(LiX)_{12}$. Campana et al. reported that cluster ions with $n = 12$, 13, 16, and 17 for $Cs^+(CsI)_n$ are relatively more stable and the relatively unstable species ($n = 14$ and 15) decompose to yield preferentially not only $n = 13$ but also $n = 12$ cluster species [19]. In the present work, the magic number of 12 is only observed for the negative cluster ions $Cl^-(LiCl)_n$ and $Br^-(LiBr)_n$ but not for other MX as shown in Table 1.

$Na^+(NaF)_n$ gives the magic number of $n = 4$, 13, 16, 17, 22, 25, 28, 31, 34, and 37. The postulated structures of cubic and hexagonal structures [3,24] for the cluster ions are depicted in Fig. 2. The magic number of $n = 3$, 6, 9, and 12 can be explicable by the hexagonal structures, while $n = 4$, 12, 13, 22, and 37 by cubic-like structures. The positive- and negative-mode EDI mass spectra for CsI are shown in Fig. 4.

In Fig. 2, the stepwise formation of cluster ions with the magic numbers of $n = 34$, 31, 28, 25, and 22 is depicted by one row each of three MX removal from the $n = 37$ cubic-like structure [11]. The incomplete row of ions is situated beside a complete terrace of ions on one side for $n = 34$, 31, 28, and 25. In fact, the relative abundances for cluster ions with the imperfect cubic-like structures with $n = 34$, 31, 28, and 25 are generally less prominent compared with the perfect cubic-like structures for $n = 37$ and 22 in this work. The magic number of $n = 19$, 16, and 13 can be also predicted by removal of one row of three MX is removed from the $n = 22$ cubic-like structure. Although $n = 17$, 16, and 13 are recognized as magic numbers for some MX, the cluster with the magic number of $n = 19$ is not observed in the present work. In our measurements, the cluster ions with complete terrace structures with $n = 4$, 13, 22, and 37 are preferentially observed as expected. It is worthwhile noting that almost the same magic numbers are observed for positive and negative cluster ions for KI and RbI.

The relative abundances for $F^-(MF)_n$ are found to be much weaker than those for $M^+(MF)_n$. This may be due to the occurrence of reaction (1) for X = F in the cluster ions.

$$X^- + CH_3COOH \rightarrow CH_3COO^- + HF \quad (1)$$

Acetic acid is a component of the charged water droplet projectiles. As far as the gas-phase reactions are concerned, only the reaction (1) for X = F is exothermic (enthalpy change of reaction: $\Delta H_r = -97$ kJ/mol) but all other reactions for X = Cl, Br, and I are endothermic.

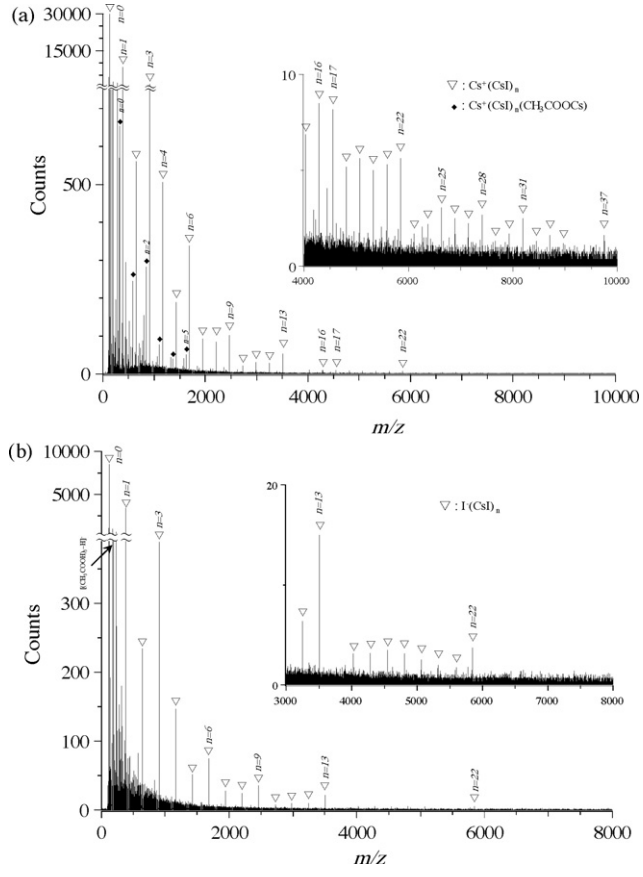

Fig. 4. Positive- and negative-mode EDI mass spectra for CsI.

4. Summary

The positive and negative EDI mass spectra for all the alkali halides (MX) are measured. The negative cluster ions $X^-(MX)_n$ with magic numbers of $n = 4$ and 12 are observed only for LiCl and LiBr. This may suggest the presence of planar structures of $(3 \times 3 \times 1)$ with $n = 4$ and of $(5 \times 5 \times 1)$ with $n = 12$. Alkali halides with smaller ionic radii do not favor the hexagonal stacked structures but prefer the cubic-like structures. The appearance of $n = 3$, 6, and 9 (i.e., stacked hexagonal structures) is common for MX with larger-ionic radii. All the magic numbers observed for $n = 37$, 34, 31, 28, 25, 22, 16, and 13 can be interpreted by the removal of each three MX pairs starting from the $n = 37$ cubic-like structure. The relatively more stable cluster ion predicted with $n = 17$ [19] is confirmed by the present work.

Acknowledgments

This work was supported by a Grant-in-Aid from the Japanese Ministry of Education, Science, and Culture (Special Coordination Funds for the Promotion of Science and Technology, no. 20,403,010) and Japan Science and Technology Agency (Development of System and Technology for Advanced Measurement and Analysis, 2007).

References

[1] F. Honda, G.M. Lancaster, Y. Fukuda, J.W. Rabalais, J. Chem. Phys. 69 (1978) 4931.
[2] J.E. Campana, T.M. Barlak, R.J. Colton, J.J. DeCorpo, J.R. Wyatt, B.I. Dunlap, Phys. Rev. Lett. 47 (1981) 1046.
[3] T.P. Martin, J. Chem. Phys. 72 (1980) 3506.
[4] T.M. Barlak, J.E. Campana, R.J. Colton, J.J. DeCorpo, J.R. Wyatt, J. Phys. Chem. 85 (1981) 3840.
[5] T.M. Barlak, J.R. Wyatt, R.J. Colton, J.J. DeCorpo, J.E. Campana, J. Am. Chem. Soc. 104 (1982) 1212.
[6] T.M. Barlak, J.E. Campana, J.R. Wyatt, R.J. Colton, J. Phys. Chem. 87 (1983) 3441.
[7] B.I. Dunlap, Surf. Sci. 121 (1982) 260.
[8] W. Ens, R. Beavis, K.G. Standing, Phys. Rev. Lett. 50 (1983) 27.
[9] I. Katakuse, T. Ichihara, H. Ito, T. Matsuo, T. Sakurai, H. Matsuda, Rapid Commun. Mass Spectrom. 2 (1988) 191.
[10] R. Pflaum, P. Pfau, K. Sattler, E. Recknagel, Surf. Sci. 156 (1985) 165.
[11] Y.J. Twu, C.W.S. Conover, Y.A. Yang, L.A. Bloomfield, Phys. Rev. B 42 (1990) 5306.
[12] L.A. Bloomfield, C.W.S. Conover, Y.A. Yang, Y.J. Twu, N.G. Phillips, Z. Phys. D 20 (1991) 93.
[13] J.E. Campana, B.I. Dunlap, Int. J. Mass Spectrom. Ion Process 57 (1984) 103.
[14] K. Hiraoka, D. Asakawa, S. Fujimaki, A. Takamizawa, K. Mori, Eur. Phys. J. D 38 (2006) 225.
[15] K. Hiraoka, K. Mori, D. Asakawa, J. Mass Spectrom. 41 (2006) 894.
[16] D. Asakawa, D.S. Fujimaki, Y. Hashimoto, K. Mori, K. Hiraoka, Rapid Commun. Mass Spectrom. 21 (2007) 1579.
[17] K. Mori, D. Asakawa, J. Sunner, K. Hiraoka, Rapid Commun. Mass Spectrom. 20 (2006) 2596.
[18] B.I. Dunlap, J.E. Campana, J. Vac. Sci. Technol. A 1 (1983) 432.
[19] J.E. Campana, R.J. Colton, J.R. Wyatt, R.H. Bateman, B.N. Green, Appl. Spectrocscopy 38 (1984) 430.
[20] J.E. Robinson, B.S. Yarlagadda, R.A. Sachs, J. Nucl. Mater. 63 (1976) 432.
[21] J.P. Biersack, D. Fink, P. Mertens, J. Nucl. Mater. 53 (1974) 194.
[22] M. Kaminsky, S.K. Das, J. Nucl. Mater. 60 (1976) 111.
[23] D.R. Lide (Ed.), Handbook of Chemistry and Physics, 84th ed., CRC Press, London, 2003–2004.
[24] T.P. Martin, J. Chem. Phys. 69 (1978) 2036.